

Supplementary Information for

Vapor Kinetic Energy for the Detection and Understanding of Atmospheric Rivers

Hing Ong¹ & Da Yang²

¹Argonne National Laboratory, Lemont, IL, USA

²University of Chicago, Chicago, IL, USA

Supplementary Note

For the readers' convenience, we have rederived the IVKE budget equations (S1 – S7) here.

These equations are identical to those presented in Methods.

Derivation of the IVKE budget

To derive the VKE prognostic equation, we start from the moisture prognostic equation:

$$\frac{\partial q}{\partial t} = -\mathbf{u} \cdot \nabla_p q - \omega \frac{\partial q}{\partial p} + S_M + S_T + S_C, \quad (\text{S1})$$

and the hydrostatic primitive momentum prognostic equation:

$$\frac{\partial \mathbf{u}}{\partial t} = -\mathbf{u} \cdot \nabla_p \mathbf{u} - \omega \frac{\partial \mathbf{u}}{\partial p} - 2\Omega \sin \vartheta \mathbf{k} \times \mathbf{u} - \frac{u \tan \vartheta}{a} \mathbf{k} \times \mathbf{u} - \nabla_p \Phi + \mathbf{F}_M + \mathbf{F}_T + \mathbf{F}_G, \quad (\text{S2})$$

where the variables are defined as follows: \mathbf{u} , horizontal velocity vector; ω , vertical motion; Φ , geopotential; Ω , planetary rotation rate; a , planetary radius; ϑ , latitude. The variables \mathbf{F}_M , \mathbf{F}_T , and \mathbf{F}_G denote apparent momentum sources or sinks due to subgrid-scale moist convection, turbulence, and gravity wave drag. The variables S_M , S_T , and S_C denote apparent moisture sources or sinks due to moist physics (including subgrid-scale moist convection, condensation, and evaporation of condensate, hereafter condensation), turbulence, and chemistry. In MERRA-2, tendencies due to dynamics refers to the combination of the first two terms on the right-hand side of Equation S1 (hereafter, S_D) and the first five terms on that of Equation S2 (hereafter, \mathbf{F}_D). Then, we derive the prognostic equation of q^2 by multiplying $2q$ to Equation S1 and applying the product rule ($2q \frac{\partial q}{\partial t} = \frac{\partial q^2}{\partial t}$):

$$\frac{\partial q^2}{\partial t} = -2q\mathbf{u} \cdot \nabla_p q - 2q\omega \frac{\partial q}{\partial p} + 2qS_M + 2qS_T + 2qS_C. \quad (\text{S3})$$

Additionally, we derive the prognostic equation of K by taking the dot product of \mathbf{u} to Equation

S2 and applying the product rule ($\mathbf{u} \cdot \frac{\partial \mathbf{u}}{\partial t} = \frac{\partial}{\partial t} \left(\frac{\mathbf{u} \cdot \mathbf{u}}{2} \right) = \frac{\partial K}{\partial t}$; $-\mathbf{u} \cdot (\mathbf{u} \cdot \nabla_p \mathbf{u}) = \mathbf{u} \cdot \nabla_p \left(\frac{\mathbf{u} \cdot \mathbf{u}}{2} \right) = -\mathbf{u} \cdot$

$\nabla_p K$; $-\mathbf{u} \cdot \omega \frac{\partial \mathbf{u}}{\partial p} = -\omega \frac{\partial}{\partial p} \left(\frac{\mathbf{u} \cdot \mathbf{u}}{2} \right) = -\omega \frac{\partial K}{\partial p}$):

$$\frac{\partial K}{\partial t} = -\mathbf{u} \cdot \nabla_p K - \omega \frac{\partial K}{\partial p} - \mathbf{u} \cdot \nabla_p \Phi + \mathbf{u} \cdot \mathbf{F}_M + \mathbf{u} \cdot \mathbf{F}_T + \mathbf{u} \cdot \mathbf{F}_G, \quad (\text{S4})$$

Adding K times Equation S3 and q^2 times Equation S4 and applying the product rule ($K \frac{\partial q^2}{\partial t} +$

$q^2 \frac{\partial K}{\partial t} = \frac{\partial q^2 K}{\partial t}$) yields the VKE prognostic equation:

$$\begin{aligned} \frac{\partial q^2 K}{\partial t} = & -q^2 \mathbf{u} \cdot \nabla_p K - q^2 \omega \frac{\partial K}{\partial p} - q^2 \mathbf{u} \cdot \nabla_p \Phi + q^2 \mathbf{u} \cdot \mathbf{F}_M + q^2 \mathbf{u} \cdot \mathbf{F}_T + q^2 \mathbf{u} \cdot \mathbf{F}_G \\ & - 2Kq \mathbf{u} \cdot \nabla_p q - 2Kq \omega \frac{\partial q}{\partial p} + 2Kq S_M + 2Kq S_T + 2Kq S_C. \end{aligned} \quad (\text{S5})$$

Taking the time derivative of Equation 2 and using the Leibniz integral rule yields a simple form of IVKE prognostic equation:

$$\frac{\partial}{\partial t} \langle q^2 K \rangle = \left\langle \frac{\partial q^2 K}{\partial t} \right\rangle + \left[\frac{q^2 K}{g} \right]_{p_B} \frac{\partial p_B}{\partial t}, \quad (\text{S6})$$

where $\langle \cdot \rangle$ denotes the following integral operator:

$$\langle \cdot \rangle \equiv -\frac{1}{g} \int_{p_B}^{p_T} (\cdot) dp.$$

Plugging Equation S5 into S6 yields the IVKE prognostic equation with complete physics:

$$\begin{aligned} \frac{\partial}{\partial t} \langle q^2 K \rangle = & \underbrace{\langle -q^2 \mathbf{u} \cdot \nabla_p K \rangle}_{\text{HAKE}} + \underbrace{\langle -q^2 \omega \frac{\partial K}{\partial p} \rangle}_{\text{VAKE}} + \underbrace{\langle -q^2 \mathbf{u} \cdot \nabla_p \Phi \rangle}_{\text{PEKE}} + \underbrace{\langle q^2 \mathbf{u} \cdot \mathbf{F}_M \rangle}_{\text{MOKE}} + \underbrace{\langle q^2 \mathbf{u} \cdot \mathbf{F}_T \rangle}_{\text{TOKE}} + \underbrace{\langle q^2 \mathbf{u} \cdot \mathbf{F}_G \rangle}_{\text{GOKE}} \\ & + \underbrace{\langle -2Kq \mathbf{u} \cdot \nabla_p q \rangle}_{\text{HAV}} + \underbrace{\langle -2Kq \omega \frac{\partial q}{\partial p} \rangle}_{\text{VAV}} + \underbrace{\langle 2Kq S_M \rangle}_{\text{COV}} + \underbrace{\langle 2Kq S_T \rangle}_{\text{TOV}} + \underbrace{\langle 2Kq S_C \rangle}_{\text{CMOV}} \\ & + \left[\frac{q^2 K}{g} \right]_{p_B} \frac{\partial p_B}{\partial t}, \end{aligned} \quad (\text{S7})$$

The acronyms are defined in Table S1. Moreover, the MERRA-2 provides nonphysical tendencies due to incorporating analysis data into winds (\mathbf{F}_A) and moisture (S_A), so we also calculate an analysis effect added to the right-hand side of Equation S7 as $\langle q^2 \mathbf{u} \cdot \mathbf{F}_A + 2KqS_A \rangle$.

Calculating the IVKE budget using MERRA-2 and ERA5 datasets

Here, we detail the methodology for assessing uncertainties in the IVKE budget using MERRA-2 data. We estimate the uncertainty of HAKE, VAKE, and PEKE using the residual of the dynamic tendency of KE (R_{DOKE}):

$$R_{\text{DOKE}} = \langle q^2 \mathbf{u} \cdot \mathbf{F}_D \rangle - \left(\langle -q^2 \mathbf{u} \cdot \nabla_p K \rangle + \langle -q^2 \omega \frac{\partial K}{\partial p} \rangle + \langle -q^2 \mathbf{u} \cdot \nabla_p \Phi \rangle \right). \quad (\text{S8})$$

We estimate the uncertainty of HAV and VAV using the residual of the dynamic tendency of vapor (R_{DOV}):

$$R_{\text{DOV}} = \langle 2KqS_D \rangle - \left(\langle -2Kq\mathbf{u} \cdot \nabla_p q \rangle + \langle -2Kq\omega \frac{\partial q}{\partial p} \rangle \right). \quad (\text{S9})$$

We estimate the uncertainty of all the other terms using the residual of the following equation (R_{total}):

$$R_{\text{total}} = \left\langle \frac{\partial q^2 K}{\partial t} \right\rangle - (\langle q^2 \mathbf{u} \cdot \mathbf{F}_D \rangle + \langle q^2 \mathbf{u} \cdot \mathbf{F}_M \rangle + \langle q^2 \mathbf{u} \cdot \mathbf{F}_T \rangle + \langle q^2 \mathbf{u} \cdot \mathbf{F}_G \rangle + \langle 2KqS_D \rangle + \langle 2KqS_M \rangle + \langle 2KqS_T \rangle + \langle 2KqS_C \rangle + \langle q^2 \mathbf{u} \cdot \mathbf{F}_A + 2KqS_A \rangle). \quad (\text{S10})$$

ERA5 does not provide \mathbf{F}_M , \mathbf{F}_T , \mathbf{F}_G , S_M , S_T , and S_C . However, MERRA-2 results suggest that \mathbf{F}_T and S_M dominate. Thus, from Equation S3 and S4, we estimate them as follows:

$$\langle q^2 \mathbf{u} \cdot \mathbf{F}_T \rangle = q^2 \frac{\partial}{\partial t} \langle K \rangle - \langle -q^2 \mathbf{u} \cdot \nabla_p K \rangle - \langle -q^2 \omega \frac{\partial K}{\partial p} \rangle - \langle -q^2 \mathbf{u} \cdot \nabla_p \Phi \rangle, \quad (\text{S11})$$

$$\langle 2KqS_M \rangle = K \frac{\partial}{\partial t} \langle q^2 \rangle - \langle -2Kq\mathbf{u} \cdot \nabla_p q \rangle - \langle -2Kq\omega \frac{\partial q}{\partial p} \rangle. \quad (\text{S12})$$

PE-to-KE conversion decomposition

The PEKE term can be decomposed into two physical processes. First, use the product rule:

$$\langle -q^2 \mathbf{u} \cdot \nabla_p \Phi \rangle = \langle q^2 \Phi \nabla_p \cdot \mathbf{u} \rangle + \langle -q^2 \nabla_p \cdot (\mathbf{u} \Phi) \rangle.$$

Then, we use the continuity equation:

$$\langle -q^2 \mathbf{u} \cdot \nabla_p \Phi \rangle = \langle -q^2 \Phi \frac{\partial \omega}{\partial p} \rangle + \langle -q^2 \nabla_p \cdot (\mathbf{u} \Phi) \rangle.$$

Then, we use the product rule again:

$$\langle -q^2 \mathbf{u} \cdot \nabla_p \Phi \rangle = \langle q^2 \omega \frac{\partial \Phi}{\partial p} \rangle + \langle -q^2 \frac{\partial}{\partial p} (\omega \Phi) \rangle + \langle -q^2 \nabla_p \cdot (\mathbf{u} \Phi) \rangle.$$

Last, we use the hydrostatic equation:

$$\langle -q^2 \mathbf{u} \cdot \nabla_p \Phi \rangle = \langle -q^2 \omega \alpha \rangle + \langle -q^2 \frac{\partial}{\partial p} (\omega \Phi) - q^2 \nabla_p \cdot (\mathbf{u} \Phi) \rangle, \quad (\text{S13})$$

where α denotes specific volume. The two brackets on the right-hand side of Equation S13 are baroclinic conversion and geopotential flux convergence. These terms largely offset each other in the composite AR (Figure S13), such that the PEKE term accounts for roughly 3% of the baroclinic conversion in terms of their contributions to the composite AR growth.

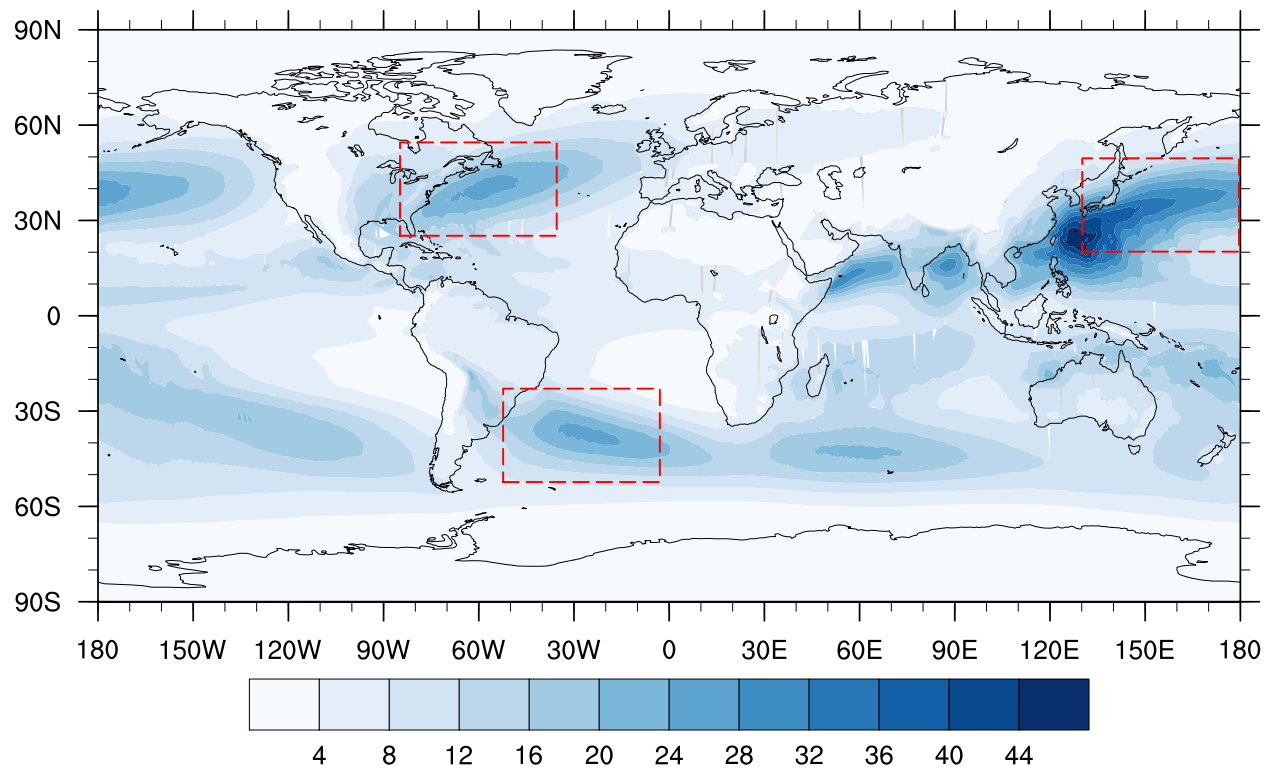


Figure S1. Sample standard deviation in time of the integrated vapor kinetic energy (IVKE) (units: kg s^{-2}) from 1980 to 2019 from MERRA-2 data. The red dash box highlights the active atmospheric river (AR) regions we selected.

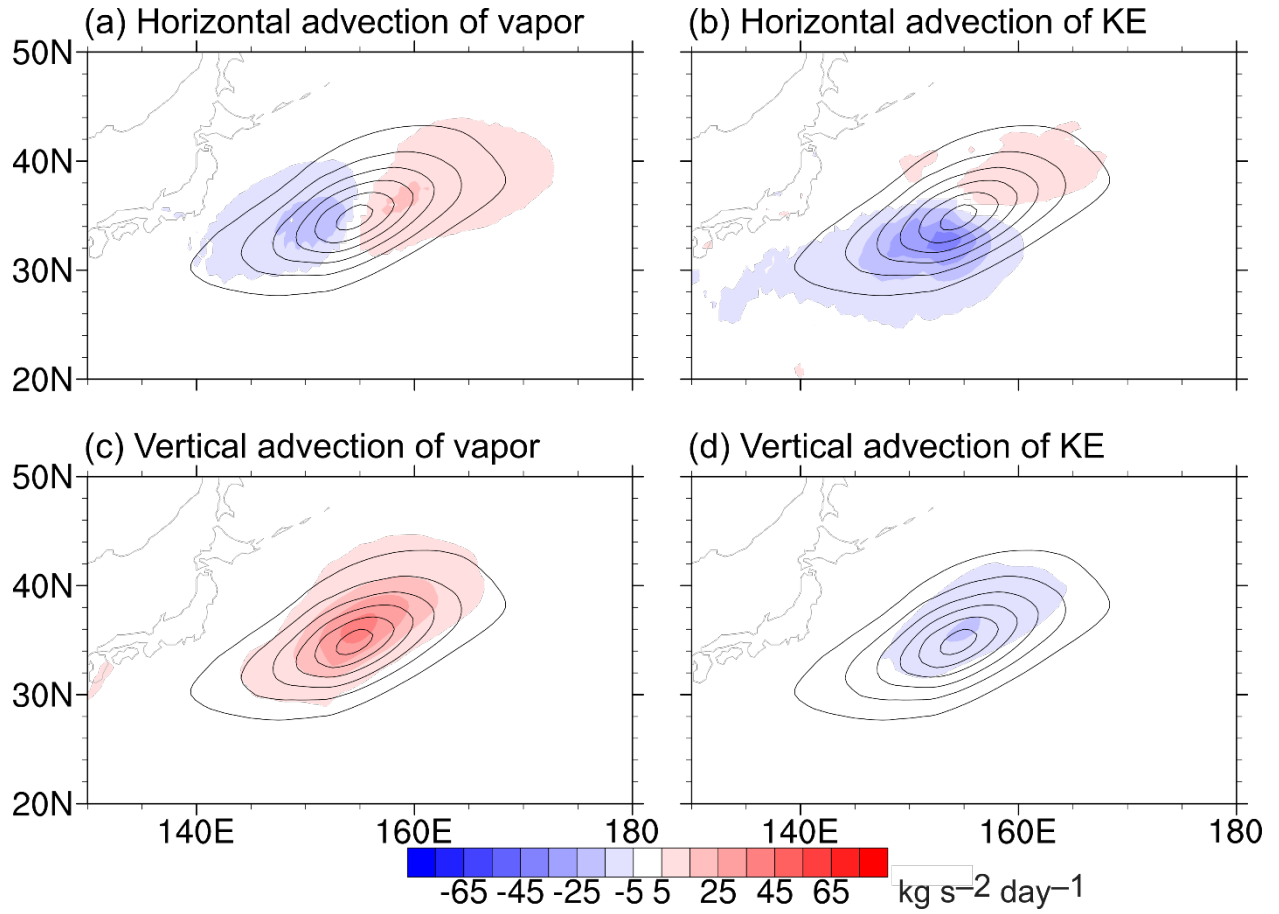


Figure S2. Map view of the integrated vapor kinetic energy (IVKE) tendencies (shading). (a) Horizontal advection of vapor. (b) Horizontal advection of KE. (c) Vertical advection of vapor. (d) vertical advection of KE. The contours represent IVKE (interval: 5 kg s^{-2}).

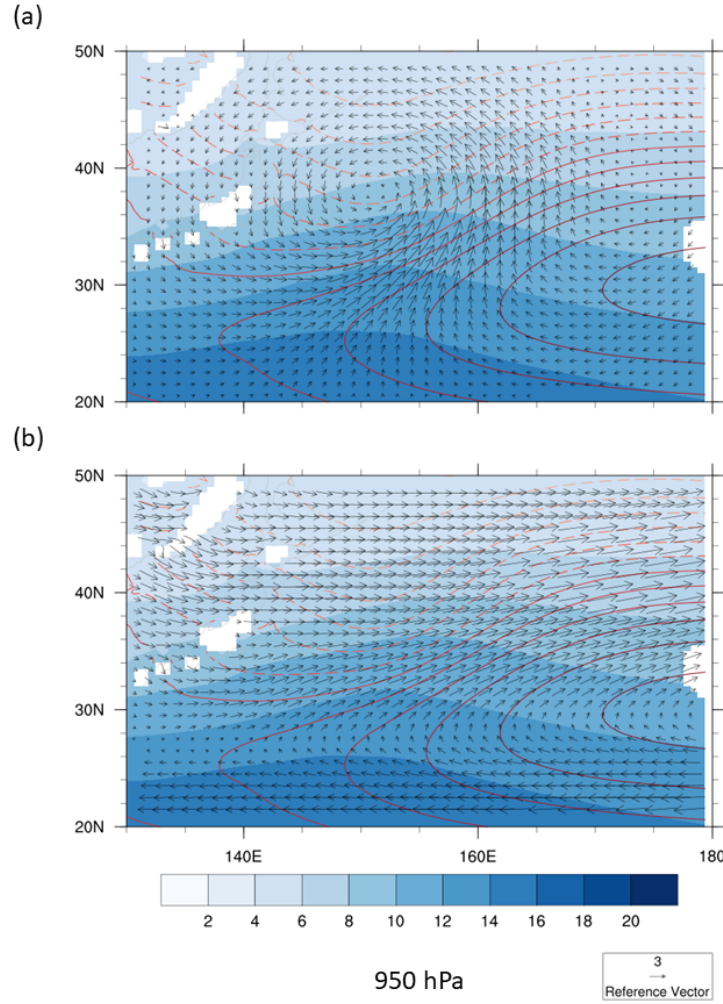


Figure S3. Atmospheric river composite at 950 hPa. (a) Winds of the composite AR. (b) Temporal mean winds. The unit for arrows is m s^{-1} . Contours represent the total geopotential height of both the composite and the temporal mean (interval: 10 m), and color shading represents the total specific humidity of both the composite and the temporal mean (units: g kg^{-1}). Solid reddish contours are higher than the areal mean geopotential height in the plotting domain, and dashed yellowish contours are lower than that. Here we use MERRA-2 data from 2010 to 2019.

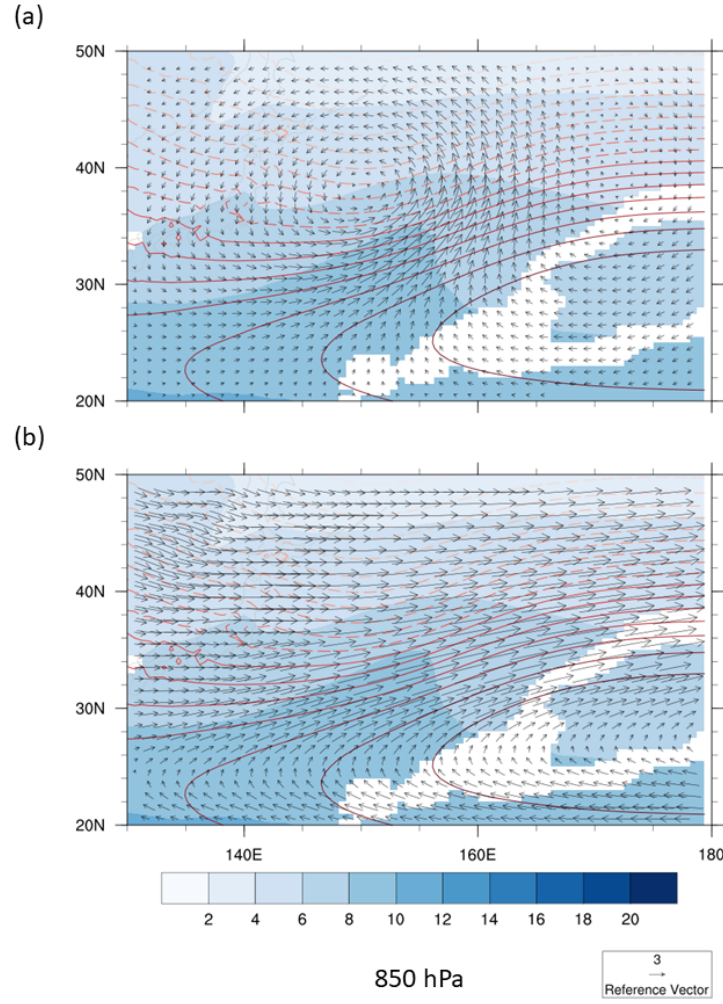


Figure S4. Atmospheric river composite at 850 hPa. (a) Winds of the composite AR. (b) Temporal mean winds. The unit for arrows is m s^{-1} . Contours represent the total geopotential height of both the composite and the temporal mean (interval: 10 m), and color shading represents the total specific humidity of both the composite and the temporal mean (units: g kg^{-1}). Solid reddish contours are higher than the areal mean geopotential height in the plotting domain, and dashed yellowish contours are lower than that. Here we use MERRA-2 data from 2010 to 2019.

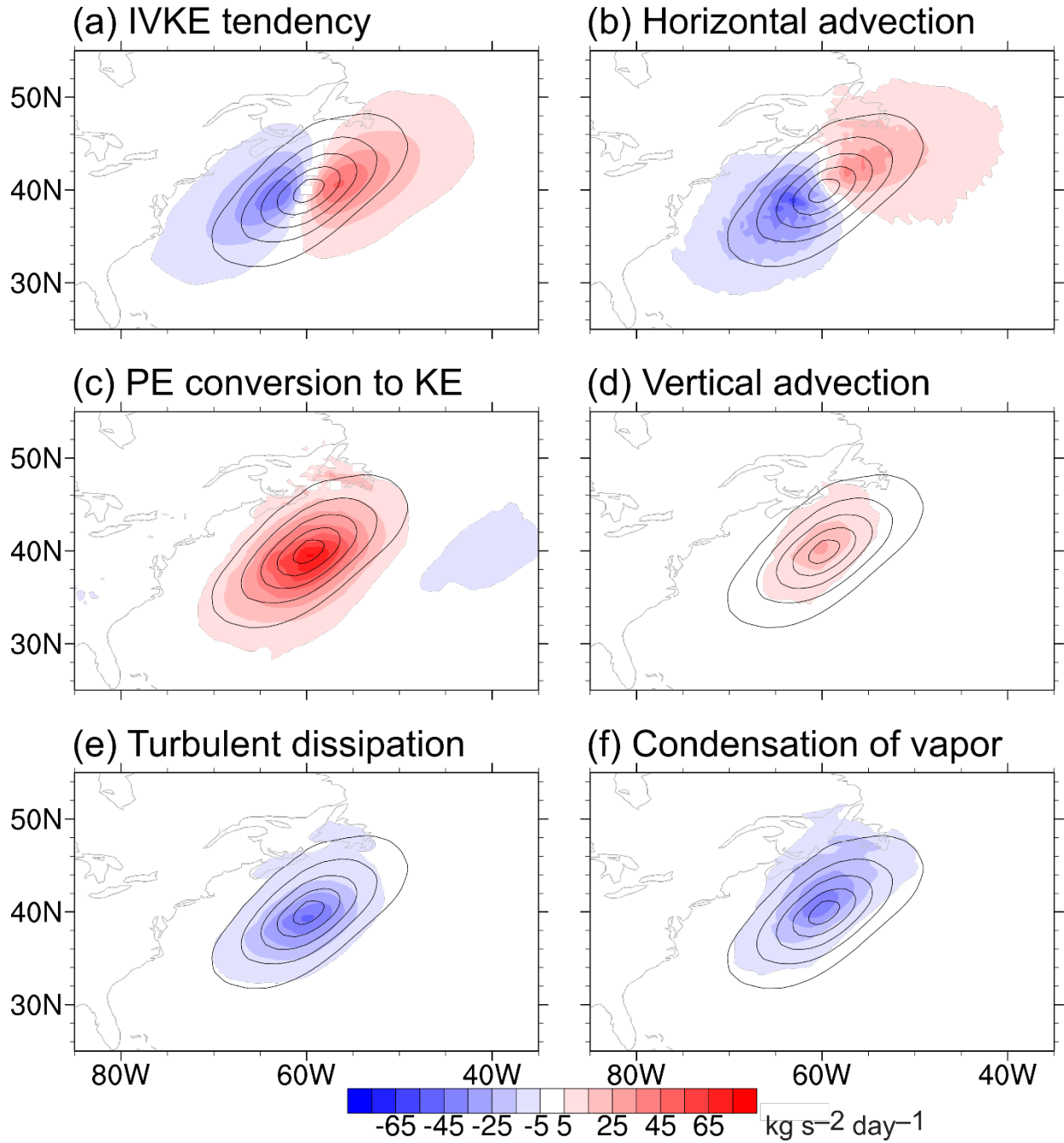


Figure S5. Atmospheric river composite in the North Atlantic. The contours are the integrated vapor kinetic energy (IVKE) (interval: 5 kg s^{-2}). The shades are IVKE tendencies: (a) total tendency, (b) horizontal advection of vapor kinetic energy (VKE), (c) potential energy conversion to kinetic energy (KE), (d) vertical advection of VKE, (e) turbulent dissipation of KE, and (f) condensation of vapor.

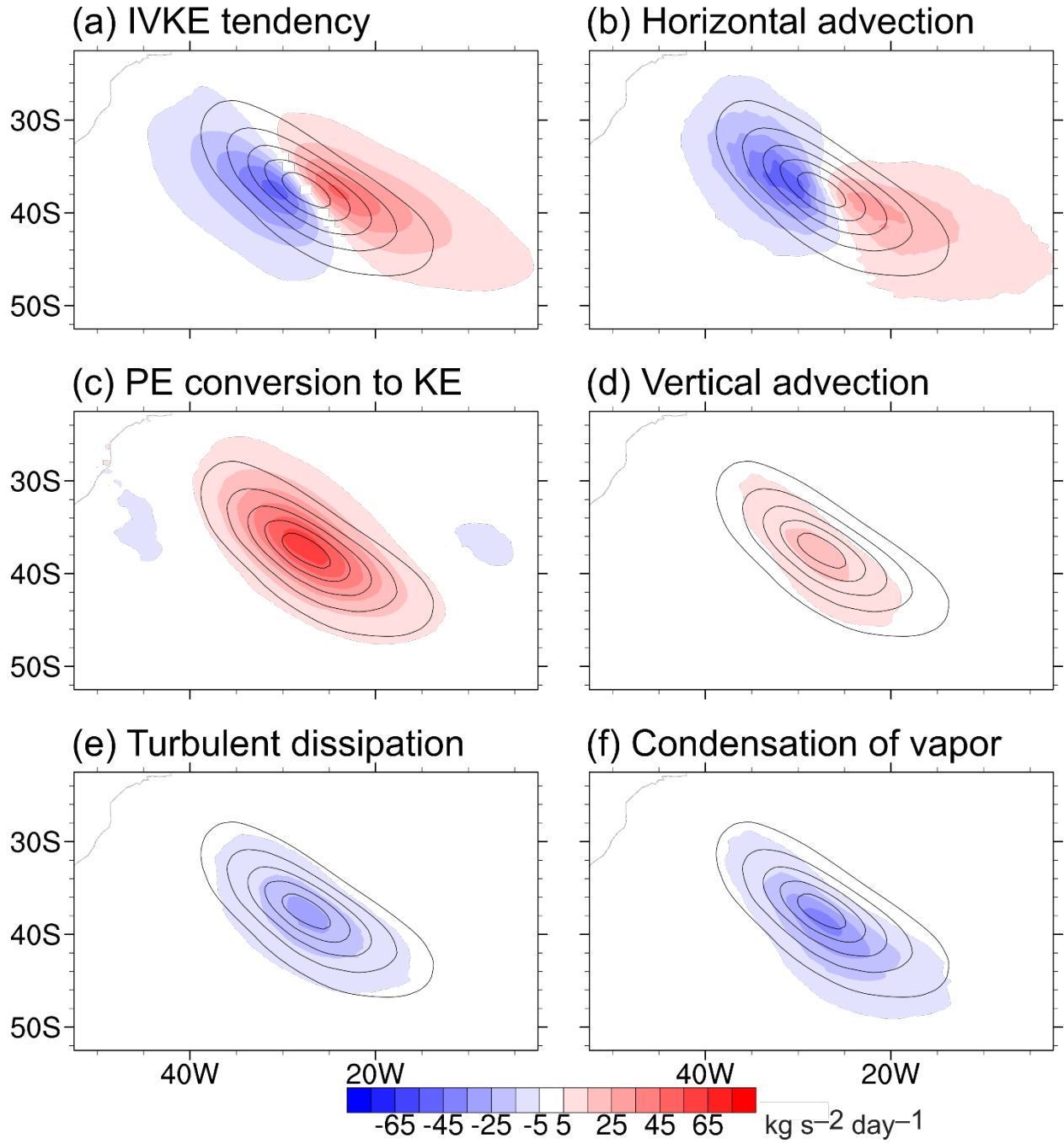


Figure S6. Atmospheric river composite in the South Atlantic. The contours are the integrated vapor kinetic energy (IVKE) (interval: 5 kg s^{-2}). The shades are IVKE tendencies: (a) total tendency, (b) horizontal advection of vapor kinetic energy (VKE), (c) potential energy conversion to kinetic energy (KE), (d) vertical advection of VKE, (e) turbulent dissipation of KE, and (f) condensation of vapor.

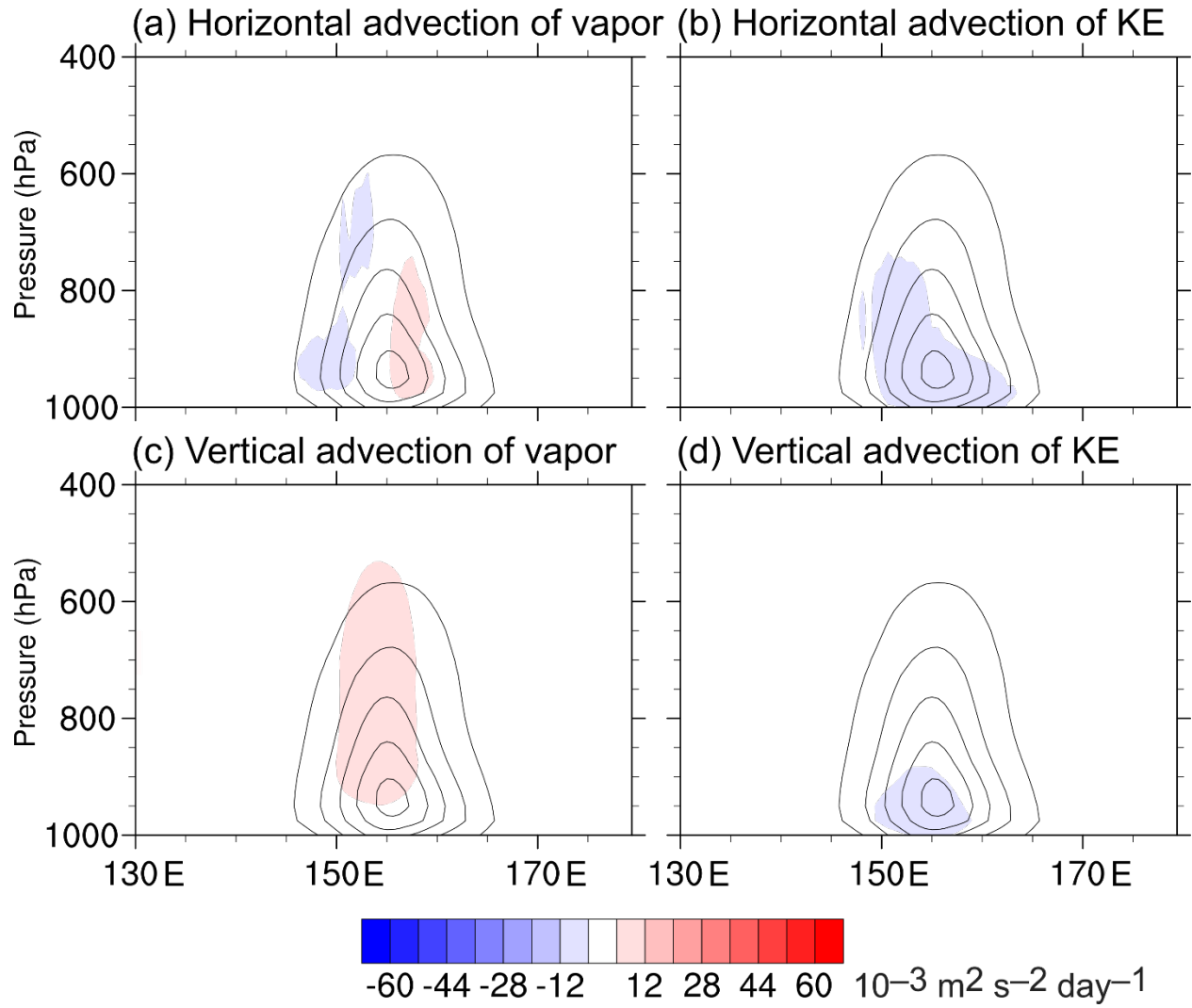


Figure S7. Vertical cross section of the atmospheric river (AR) composite, averaged between 34.5°N and 35.5°N . The contours are vapor kinetic energy (VKE) (interval: $2 \times 10^{-3} \text{ m}^2 \text{ s}^{-2}$). The shades are VKE tendencies: (a) horizontal advection of vapor, (b) horizontal advection of KE, (c) vertical advection of vapor, and (d) vertical advection of KE.

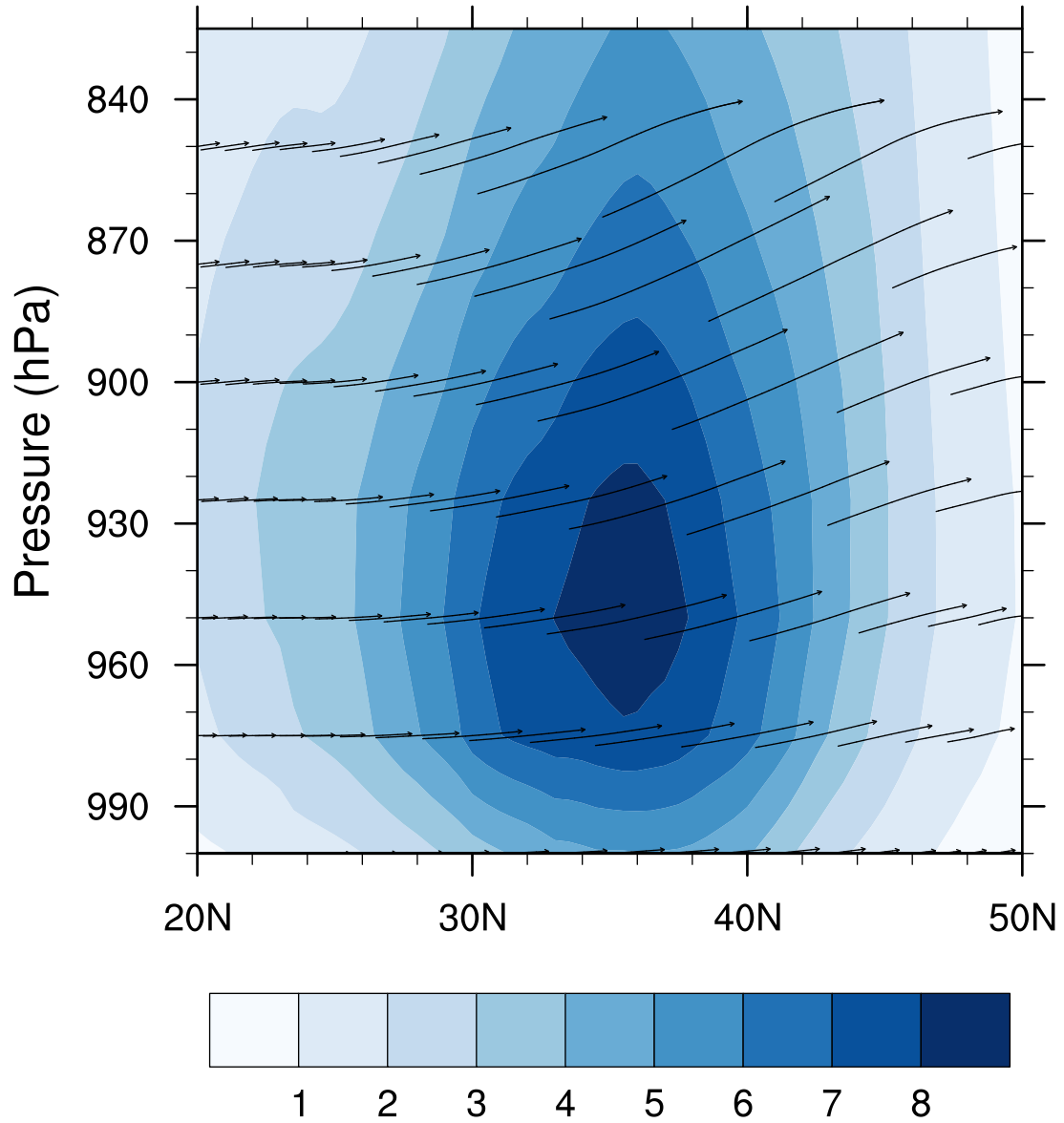


Figure S8. Vertical cross section of the atmospheric river composite averaged between 154.5°E and 155.5°E. Anomalous vapor kinetic energy (shades, units: $10^{-3} \text{ m}^2 \text{ s}^{-2}$) and anomalous air motion (arrows).

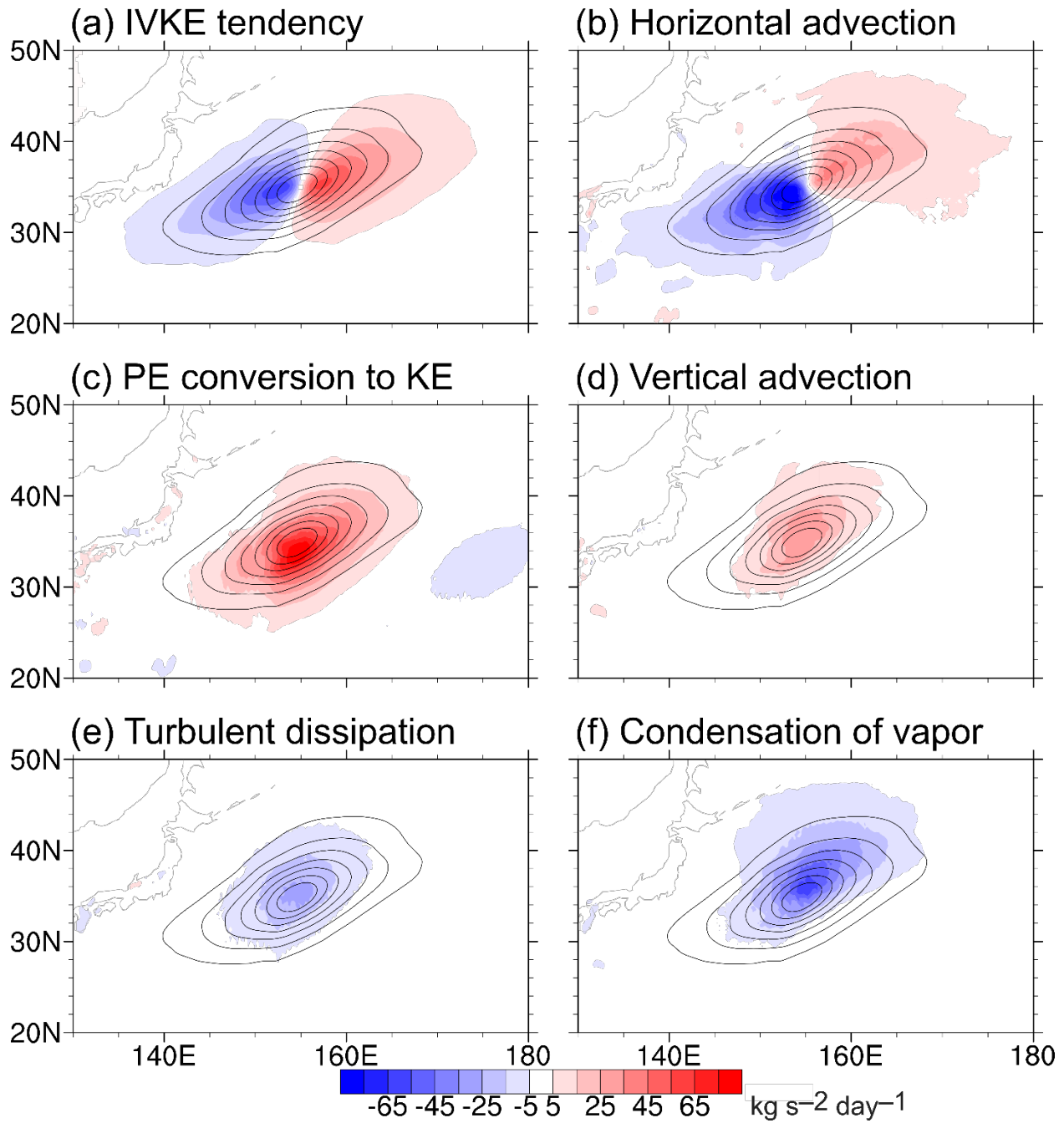


Figure S9. Plan view of the atmospheric river composite using ERA5 data. The contours are the integrated vapor kinetic energy (IVKE) (interval: 5 kg s^{-2}). The shades are IVKE tendencies: (a) total tendency, (b) horizontal advection of vapor kinetic energy (VKE), (c) potential energy conversion to kinetic energy (KE), (d) vertical advection of VKE, (e) turbulent dissipation of KE, and (f) condensation of vapor.

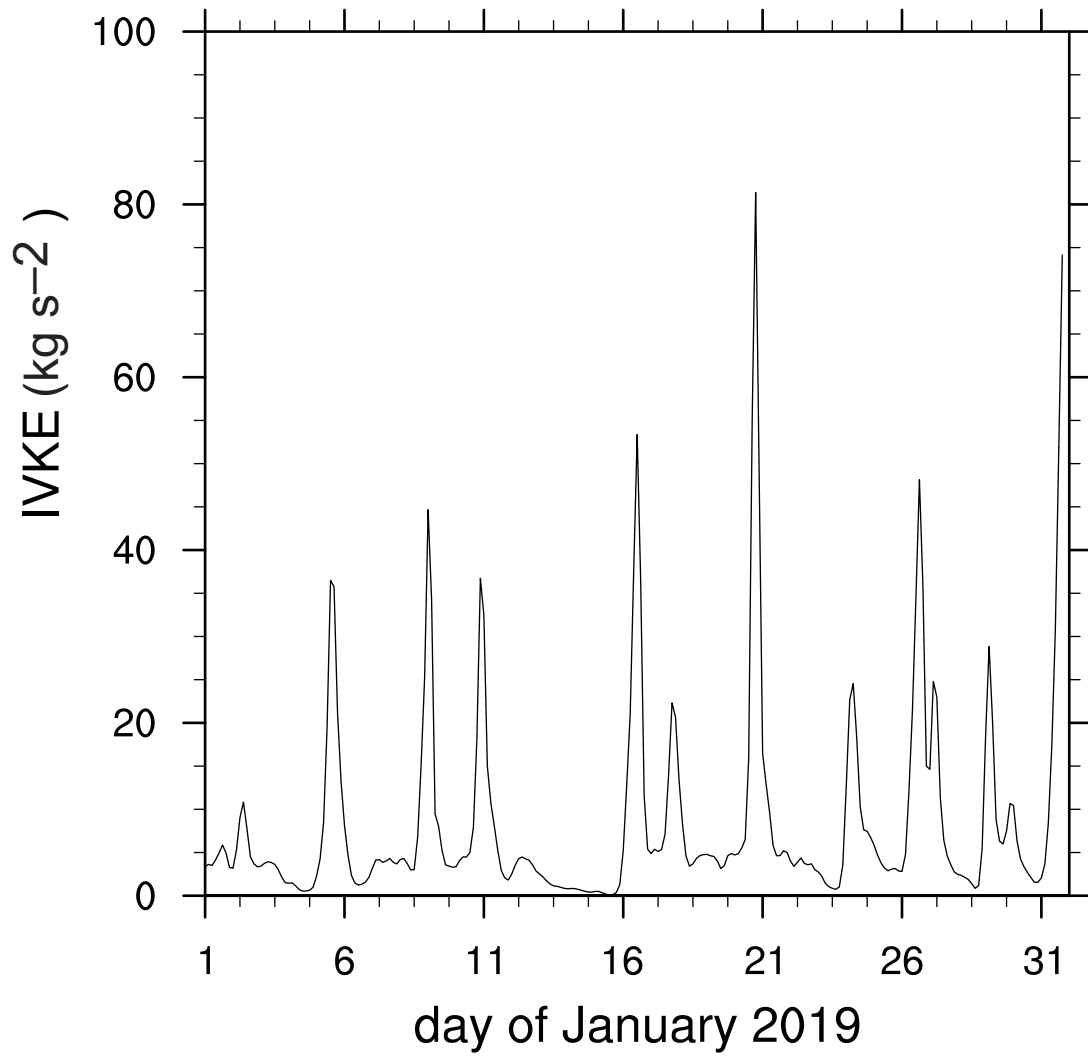


Figure S10. Three-hourly time series of IVKE in the $1^{\circ} \times 1^{\circ}$ box centered at 155°E 35°N in January 2019 from MERRA-2 data.

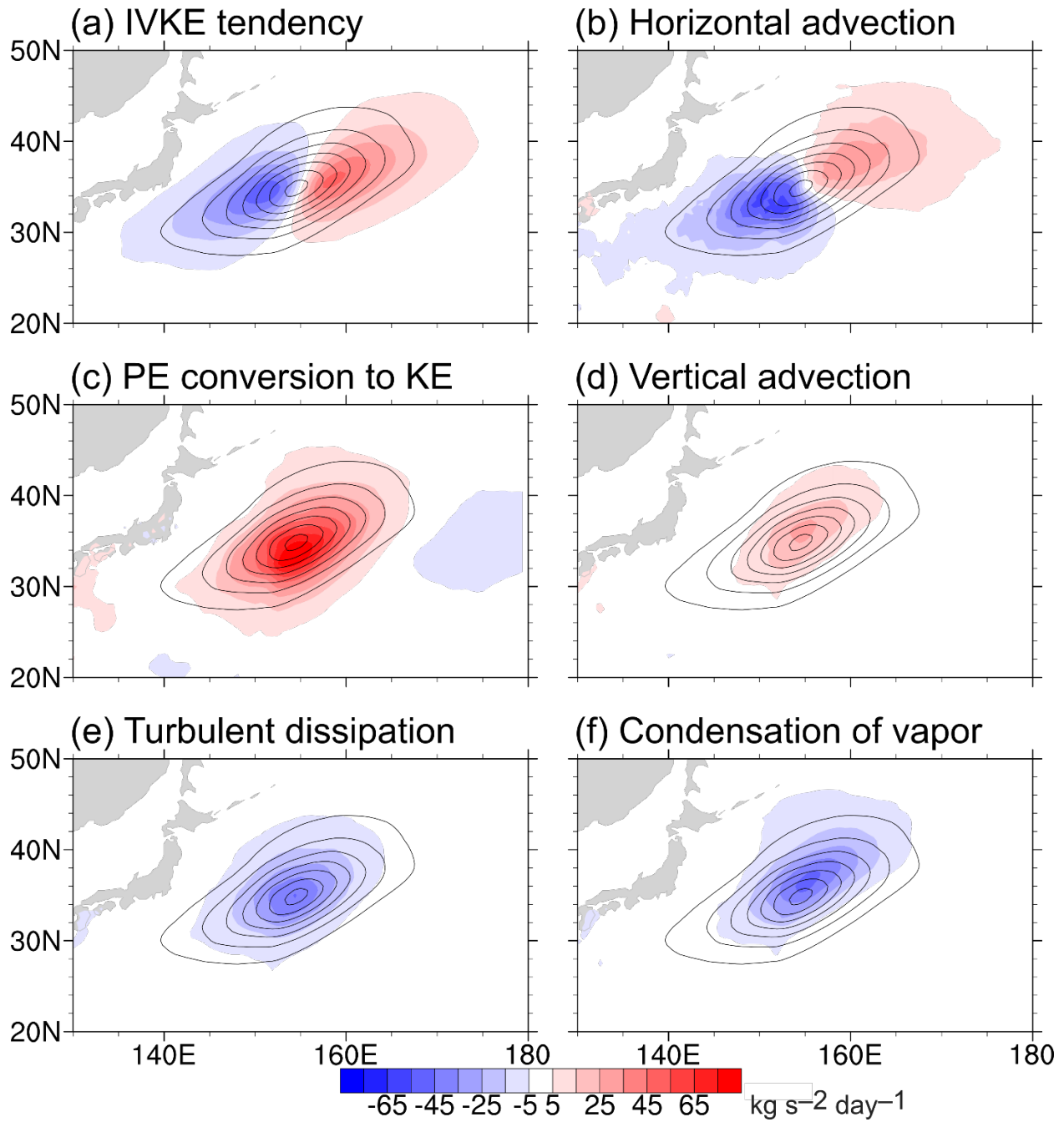


Figure S11. Plan view of the atmospheric river composite using MERRA-2 data. This calculation excludes time steps when atmospheric rivers are not detected in the $1^\circ \times 1^\circ$ box centered at 155°E 35°N using the TempestExtremes.

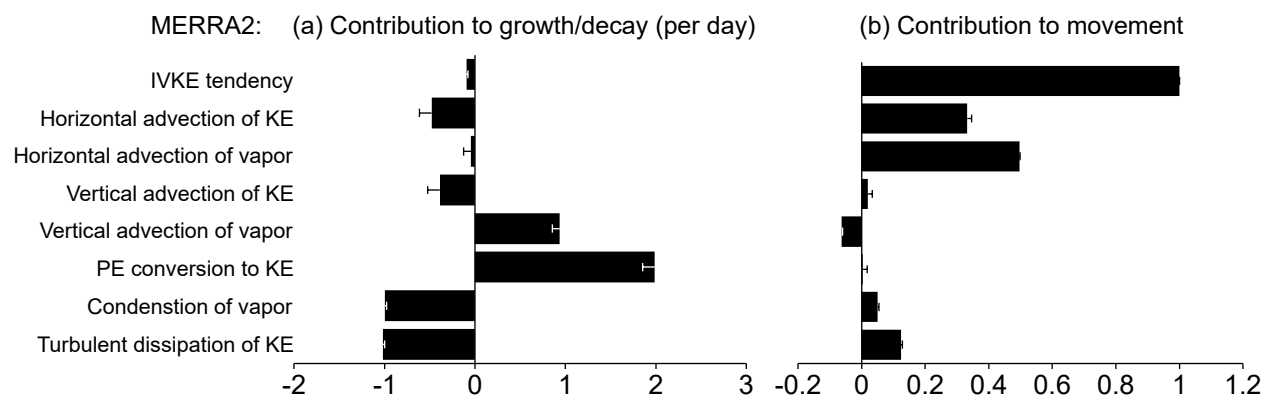
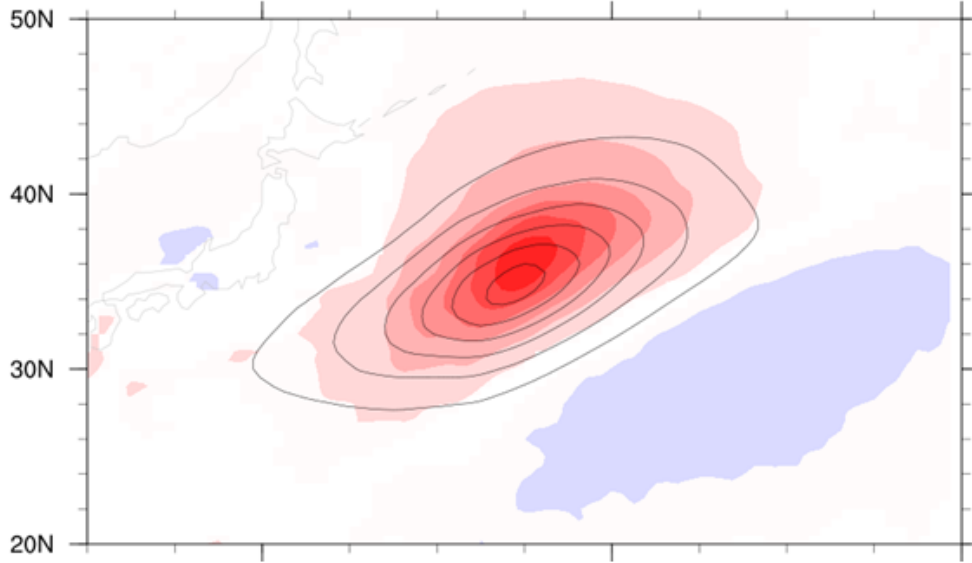


Figure S12. The integrated vapor kinetic energy (IVKE) budget for the atmospheric river composite over the analysis domain of 135°E to 175°, 25°N to 45°N. The error bars represent the residuals (Equations S8 to S10).

(a) Baroclinic conversion



(b) Geopotential flux convergence

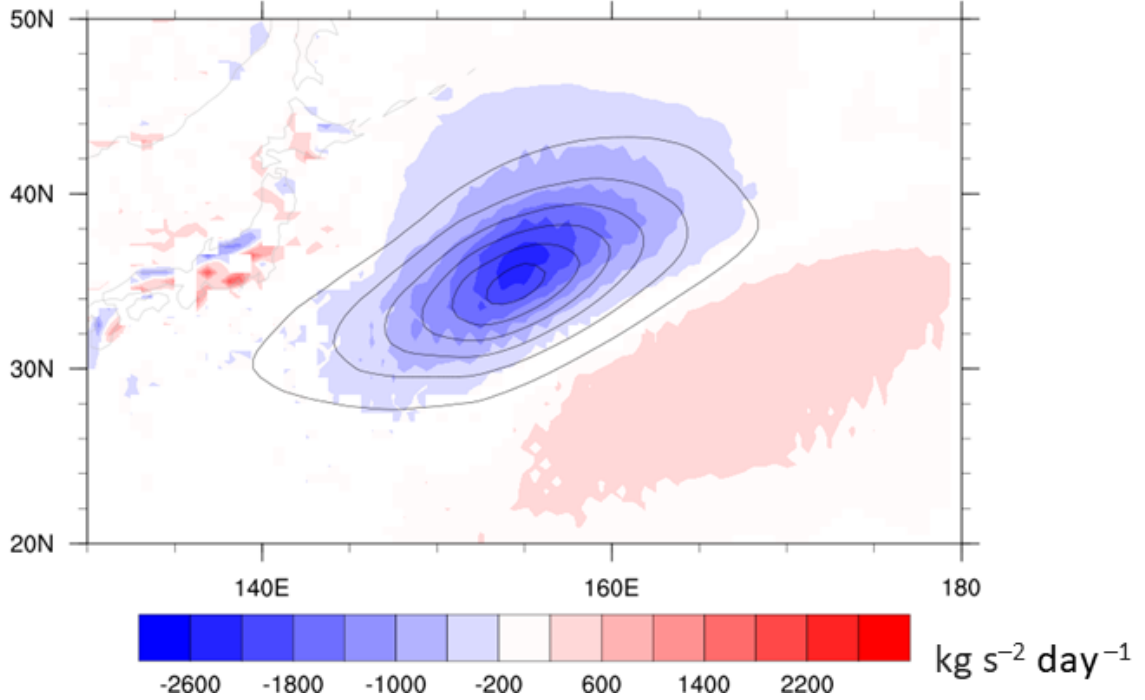


Figure S13 Decomposition of the potential energy conversion to kinetic energy (PEKE) The shading denotes IVKE tendencies due to (a) baroclinic conversion, and (b) geopotential flux convergence.

Table S1. Contribution of physical processes to the composite AR in Figure 2 using MERRA-2.

	Growth or decay (%) ¹	Movement (%) ²
IVKE tendency	-3.1	100.0
Horizontal advection of KE (HAKE)	-15.9	+33.6
Vertical advection of KE (VAKE)	-12.8	+2.0
Potential energy conversion to KE (PEKE)	+65.8	+0.1
Turbulent dissipation of KE (TOKE)	-33.7	12.3
Moist convection tendency of KE (MOKE)	+0.7	-0.6
Gravity wave drag of KE (GOKE)	0.0	0.0
Horizontal advection of vapor (HAV)	-1.4	+49.7
Vertical advection of vapor (VAV)	+31.1	-6.3
Condensation of vapor (COV)	-33.1	+5.0
Turbulent tendency of vapor (TOV)	+2.3	-4.1
Chemistry tendency of vapor (CMOV)	0.0	0.0
Surface pressure tendency effect (SPTE)	-0.6	-1.1
Analysis effect	+2.2	+2.0
Residual (DOKE, see Eq. S8)	-4.5	+1.4
Residual (DOV, see Eq. S9)	-2.7	+0.2
Residual (total, see Eq. S10)	+0.6	+0.4

¹ Percentage to the sum of all the physical sources (*i.e.*, positive terms except analysis effect and residual)² Percentage to the IVKE tendency